



Evaluation of reconstructed sea surface temperatures based on U_{37}^K from sediment surface samples of the North Pacific

Lars Max ^{a,b,*}, Lester Lembke-Jene ^a, Jianjun Zou ^{c,d}, Xuefa Shi ^{c,d}, Ralf Tiedemann ^a

^a Alfred Wegener Institute Helmholtz Centre for Polar and Marine Research, Bremerhaven, Germany

^b MARUM - Center for Marine Environmental Sciences and Faculty of Geosciences, University of Bremen, Leobener Str. 8, 28334, Bremen, Germany

^c First Institute of Oceanography, Ministry of Natural Resources, Qingdao, 266061, China

^d Laboratory for Marine Geology, Qingdao National Laboratory for Marine Science and Technology, Qingdao, 266061, China



ARTICLE INFO

Article history:

Received 19 May 2020

Received in revised form

15 July 2020

Accepted 19 July 2020

Available online 5 August 2020

Keywords:

North Pacific

Bering Sea

Okhotsk Sea

Paleoclimatology

Sediment trap

Sediment surface samples

Marine biomarkers

Alkenone

Sea surface temperature

Seasonality

ABSTRACT

The alkenone unsaturation index (U_{37}^K) as proxy for sea surface temperature (SST) is an important tool in paleoclimatology for reconstructing past ocean temperature variability. Typically, U_{37}^K recorded in marine surface sediments shows a linear correlation with modern mean annual SST. However, in high-latitude oceanic regions, such as the subpolar Pacific, U_{37}^K -based SSTs do overestimate the mean annual temperature by up to 6 °C, potentially leading to obscured paleoclimatic information drawn from stratigraphic U_{37}^K -records. The reason for this “warm bias” is still not well understood. Here, we present a compilation of 97 sediment surface samples from Multicores collected in the Bering Sea, the Okhotsk Sea and the North Pacific to evaluate the alkenone-temperature proxy against observational data from the North Pacific. Sediment surface samples were analysed for alkenones and the derived U_{37}^K -indices converted to water temperatures using different calibration equations established in the literature. U_{37}^K -based SSTs were then compared to instrumental SST data, as well as modern alkenone flux data from sediment traps in the North Pacific. Our results confirm that most U_{37}^K -based SSTs from the subpolar Pacific are 2–6 °C too warm compared to instrumental mean annual SSTs for calibrations applied. However, with an uncertainty at the level of ±1.5 °C or less reconstructed SSTs fit quite well to modern autumn temperatures north of the Subarctic Front (SAF), when maximum export flux of alkenones to the seafloor is indicated by sediment trap data. South of the SAF, reconstructed SSTs largely mimic the modern mean annual SST signal with an uncertainty of ±1.5 °C or less, which is likely due to the attenuation of seasonality and longer growth season of coccolithophorids according to sediment trap data. Our study further demonstrates that U_{37}^K , when seasonality in alkenone production and export are known and considered, is able to provide reasonable estimates of SSTs in modern high-latitude ocean settings. We conduct a case study using available alkenone time-series derived from a sediment core collected from the south-western Okhotsk Sea to better understand the potential effect of seasonality in alkenone production on stratigraphic U_{37}^K -record in the subpolar Pacific. The case study from the Okhotsk Sea indicates that even a small shift in seasonality may lead to strongly biased SSTs with broader regional implications for paleoclimate reconstructions in high-latitude ocean settings.

© 2020 The Author(s). Published by Elsevier Ltd. This is an open access article under the CC BY license (<http://creativecommons.org/licenses/by/4.0/>).

1. Introduction

Since the unsaturation ratio (U_{37}^K) of long-chain C₃₇ alkenones produced by specific marine haptophycean algae was introduced as proxy for sea surface temperature (SST) about 30 years ago (Brassell et al., 1986; Prahl and Wakeham, 1987), it has become a major tool in paleoceanography to study past SST variability of the global

* Corresponding author. MARUM - Center for Marine Environmental Sciences and Faculty of Geosciences, University of Bremen, Leobener Str. 8, 28334, Bremen, Germany.

E-mail address: lmax@marum.de (L. Max).

ocean. Empirically determined on laboratory culture experiments, the U_{37}^K index is defined as relative abundance of di- and triunsaturated C_{37} alkenones biosynthesized by the marine haptophycean algae *Emiliania huxleyi* (*E. huxleyi*):

$$(1) U_{37}^K = [C37:2]/[C37:2 + C37:3] \text{ (Prahl and Wakeham, 1987)}$$

A linear relationship between U_{37}^K and SST has been described with following equation:

$$(2) U_{37}^K = 0.034T + 0.039 \text{ (Prahl et al., 1988).}$$

Several calibration studies between alkenone indices and SST using other algal culture, water-column particles and marine sediments further confirmed the relationship between the U_{37}^K index and SST (e.g. Sikes et al., 1991; Rosell-Melé et al., 1995; Sikes et al., 1997; Sonzogni et al., 1997; Conte et al., 1998; Rosell-Melé, 1998). Müller et al. (1998) were among the first to provide a global core-top calibration of U_{37}^K derived from 370 marine surface samples spanning the world ocean between 60°N and 60°S . The global core-top calibration shows a remarkably strong linear correlation with mean annual SST ($U_{37}^K = 0.033T + 0.044$; $r^2 = 0.958$), but more importantly is virtually identical to the initial U_{37}^K calibration based on laboratory culture studies (Prahl and Wakeham, 1987; Prahl et al., 1988), attesting to the general applicability of alkenones to reconstruct past SST from marine sediments.

Given its general applicability the U_{37}^K index or “alkenone thermometer” has become a major tool for reconstructing past SSTs. The use of this algal proxy has allowed to put important constraints on past SST variability from various timescales and regions, e.g. from the tropical to subtropical regions of the Atlantic (e.g. Villanueva et al., 1998; Bard et al., 2000; Naafs et al., 2010), Pacific (e.g. Seki et al., 2002; Yamamoto et al., 2004; Herbert et al., 2010) and Indian Ocean (e.g. Bard et al., 1997; Wang et al., 2013) to the high latitudes of the North Atlantic (e.g. Marchal et al., 2002; Bauch et al., 2011; Naafs et al., 2013), the North Pacific (e.g. Harada et al., 2014; Max et al., 2012; Max et al., 2014) and Southern Ocean (e.g. Ikehara et al., 1997; Martinez-Garcia et al., 2009; Ho et al., 2012).

Although the strong statistical relationship between U_{37}^K and mean annual SST holds in many regions of the world ocean, several studies reported apparent discrepancies between reconstructed SST and mean annual SST, for instance in subpolar ocean regions (e.g. Sikes et al., 1997; Rosell-Melé et al., 2000; Prahl et al., 2010; Méheust et al., 2013). For the subpolar Pacific, alkenone-derived SST estimates using the global core-top calibration of U_{37}^K notoriously overestimate (warm bias) modern mean annual SST (Prahl et al., 2010; Méheust et al., 2013). Prahl et al. (2010) reported a significant and systematic offset between alkenone SSTs and mean annual SST from Multicores of SE Alaska ($55\text{--}61^\circ\text{N}$), where reconstructed SSTs were up to 4°C higher than the instrumental mean annual SSTs. One factor that may obscure U_{37}^K -based SSTs estimates is redox-dependent, compound-selective degradation of C_{37} alkenones that can lead to significant alteration of the U_{37}^K -index after deposition (e.g. Hoefs et al., 1998; Gong and Hollander, 1999; Rontani et al., 2008; Rontani et al., 2013). Prahl et al. (2010) looked for epoxides indicative of selective alkenone degradation to further understand the conspicuous SSTs from the U_{37}^K -signal. In SE Alaskan sediments, selective alkenone degradation by aerobic

bacterial processes were identified leading to an average “warming” effect of $\sim 1.4^\circ\text{C}$. However, it has been shown that even after adjustment of this potential diagenetic “warming” effect, U_{37}^K -based SSTs are still too warm and do not reflect the mean annual SST (Prahl et al., 2010). A similar systematic warm bias in U_{37}^K and mean annual SST has been reported from analysis of surface sediments in the Bering Sea and subpolar Northeast Pacific (Méheust et al., 2013).

In general, environmental factors such as non-thermal physiological stress to e.g. changes in nutrient concentrations may also affect to a variable amount the U_{37}^K -signal preserved in marine sediments (e.g. Epstein et al., 1998; Yamamoto et al., 2000). Based on culturing experiments of *E. huxleyi* it has been shown that U_{37}^K -values also vary with nutrient availability and growth stage (Epstein et al., 1998). However, Herbert (2003) argued that, in most cases, these factors produce errors at the level of 1.5°C or less that are not larger than the mean standard error of the entire regression for the global ocean calibration. Lateral transport of allochthonous alkenones is another factor that may obscure U_{37}^K values and has been proposed to explain anomalous SSTs in the high-latitude North Atlantic (Rosell-Melé et al., 2000). Hence, all these different factors may randomly affect the preserved U_{37}^K -signal by a variable amount depending upon regional oceanographic conditions, however, do not fully explain the non-random and systematic departure of the U_{37}^K proxy from mean annual SST that has been reported from the subpolar Pacific.

The seasonal production and export of alkenones is another particularly important aspect in subpolar ocean settings (e.g. Sikes et al., 1997; Harada et al., 2006a; Seki et al., 2007). For the Southern Ocean, Sikes et al. (1997) combined water column data with sedimentary temperature estimates and concluded that alkenone distributions are seasonally biased towards summer, and reconstructed SSTs better fit to times when alkenone flux to the sea floor is high. How seasonality of coccolithophorid blooms (alkenone flux) in the subpolar Pacific is related (or not) to the U_{37}^K -temperature signal recorded in marine sediments is still not evaluated. Given the importance of U_{37}^K index in paleoclimatology further evaluation of the “alkenone thermometer” from regions where non-random, regional variations in the core-top calibration of U_{37}^K -temperature vs mean annual SST exists are essential to enhance the quality of paleoclimatic interpretations drawn from such records (Rosell-Melé and Prahl, 2013).

Here, we report results from a compilation of 97 sediment surface samples from Multicores of the Bering Sea, the Okhotsk Sea and the North Pacific to further evaluate the U_{37}^K index as proxy for SST. This compilation consists of 42 new surface sediment samples from the subpolar Pacific analysed in this study. Additional data comes from published biomarker studies of Multicores recovered from coastal and marine sites throughout SE Alaska (16 samples, Prahl et al., 2010) and from R/V Sonne expedition SO202 to the eastern Bering Sea and North Pacific (39 samples, Gersonde et al., 2012; Méheust et al., 2013). Sediment surface samples were analysed for alkenones and the U_{37}^K -index converted to water temperatures using different calibration equations established in the literature. In a next step, instrumental SST data and published modern alkenone flux data from sediment traps are compared to further evaluate reconstructed alkenone temperatures against observational SST data of the North Pacific.

2. Regional setting

2.1. Surface currents

The surface circulation of the North Pacific follows a cyclonic circulation pattern that governs the rate of heat and nutrient exchange between different ocean regions of the study area (Fig. 1). The subarctic front (SAF) separates the study area into a northern (subpolar) and southern (transitional) zone of the North Pacific. Study sites south of the SAF are situated within the Kuroshio – North Pacific Current system. Intensity of the east–west thermal fronts (the SAF and the Subarctic Boundary) are very pronounced, in particular on the western part of the North Pacific (Roden et al., 1982). North of the SAF in the subpolar Pacific, the main circulation regime consists of two prominent counter-clockwise circulating systems, the Alaska Gyre in the Northeast Pacific and the Western Subarctic Gyre (WSAG). The Alaskan Stream, a northern boundary current, carries relatively warm water masses from the Alaska Gyre along the Aleutian Island Arc into the WSAG, thereby flowing into the Bering Sea through several passes between the Aleutian Islands (Fig. 1). In the Bering Sea, the surface currents of the Aleutian North Slope Current (ANSC) and Bering Slope Current (BSC) describe a large-scale counter-clockwise surface circulation. Surface waters leave the Bering Sea through the Kamchatka Strait back into the North Pacific via the East Kamchatka Current (EKC) and, to some extent, via Bering Strait into the Arctic Ocean (Stabeno et al., 1999). A part of the EKC enters the Okhotsk Sea through the Kurile Island Arc, thereby influencing surface waters of the Okhotsk Gyre (Fig. 1). The Kamchatka Current (KAC) describes the inflow into the Okhotsk Sea, the East Sakhalin Current (ESC) on the western flank of the Okhotsk Sea transports waters back to the North Pacific. Further to the south, the Oyashio Current (OC) develops and brings cold and nutrient-rich waters back to the North Pacific. The confluence of the Kuroshio Current (KC) that carries warm and

saline waters to the north and cold and nutrient-rich OC happens next to the southern tip of Hokkaido.

2.2. Sea surface temperatures, sea-ice variability and marine productivity

The high latitudes of the North Pacific are characterized by pronounced seasonal variability in SST and sea-ice distribution, which is tightly coupled to the interplay between the Siberian High and Aleutian Low pressure systems (e.g. Niebauer et al., 1998). During winter, the Aleutian Low strengthens and moves south-eastward, thereby leading to advection of cold air masses from the Arctic to the subpolar Pacific (Sekine, 1988) that causes strong sea surface cooling, intense winter mixing of nutrient-rich subsurface waters and the expansion of sea-ice in the Bering Sea and Okhotsk Sea. During this time interval sea-ice covers up to 75% of the Okhotsk Sea from winter to spring (Yang and Honjo, 1996). In contrast, winter sea-ice cover in the Bering Sea is rather moderate and confined to the shelf areas, thus most of the Bering Sea stays ice-free the entire year. During the summer months, increased insolation and weakening of the Aleutian Low lead to warmer SSTs, strong upper ocean stratification and ice-free conditions in the marginal seas (Ohtani et al., 1972). The seasonal temperature difference is quite pronounced in the study area, which typically ranges from 0 to 2 °C in winter to 8–10 °C in summer north of the SAF and from 10 to 15 °C in winter to 20–25 °C during summer months south of the SAF (Locarnini et al., 2006).

In the subpolar Pacific, marine productivity and export flux patterns to the ocean interior are intimately linked to seasonal variations in meteorological and physical oceanographic conditions. (Honda et al., 2002; Harada et al., 2003, 2006a; Nakatsuka et al., 2004; Seki et al., 2007; Tsutsui et al., 2016). The seasonal pattern of export production in the marginal seas follows the seasonal sea-ice pattern because phytoplankton production is heavily

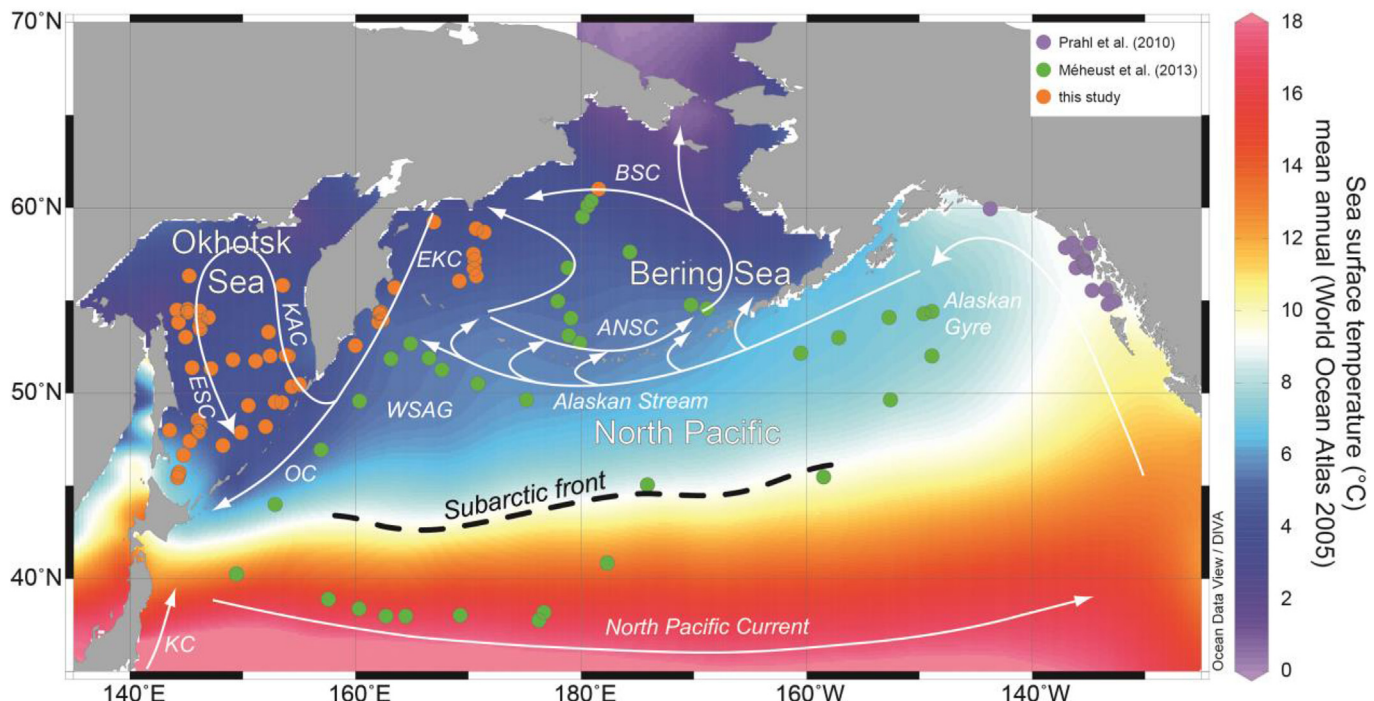


Fig. 1. Distribution of North Pacific Multicore surface samples (coloured spots) with surface circulation (white arrows) and gridded instrumental mean annual temperature data derived from World Ocean Atlas 2005 (WOA05; Locarnini et al., 2006): ANSC = Aleutian North Slope Current; BSC = Bering Slope Current; EKC = East Kamchatka Current; ESC = Sakhalin Current; KAC = Kamchatka Current; KC = Kuroshio Current; OC = Oyashio Current. This figure was generated with Ocean Data View (Schlitzer, 2015).

depressed during the sea-ice period (e.g. Honda et al., 2002). Results from sediment trap time-series of the subpolar Northwest Pacific and Okhotsk Sea show a first maximum in biogenic productivity that occurs during spring to early summer and is related to extensive diatom blooms (Honda et al., 2002; Seki et al., 2007). In the subpolar Northwest Pacific blooms of *E. huxleyi* typically occur from late summer to autumn with maximum flux of alkenones observed during October–November (Harada et al., 2006a). In the Bering Sea and Okhotsk Sea *E. huxleyi* blooms are restricted to the autumn season (September–November), suggesting that a large proportion of alkenones are synthesized during limited periods (Harada et al., 2003; Seki et al., 2007; Tsutsui et al., 2016). Sediment trap data south of the SAF in the mid-latitude Northwest Pacific show extended blooms of *E. huxleyi* that rise from the beginning of spring (March) and remain high until autumn (November) (Yamamoto et al., 2007).

3. Material and methods

The comprehensive dataset presented here spans for the first time all major parts of the transitional to subpolar Pacific including the Bering Sea and Okhotsk Sea (Fig. 1). We analysed 42 new surface sediment samples (typically 0–1 cm) for alkenones that were collected with Multicores during several expeditions to the Okhotsk Sea, Bering Sea and North Pacific from 1997 to 2013: R/V Akademik M.A. Lavrentyev cruise LV27 (Nürnberg et al., 1997); R/V Akademik M.A. Lavrentyev cruise LV28 (Biebow and Hütten, 1999); R/V Marshal Gelovany cruise GE99 (Biebow et al., 2000); R/V Akademik M.A. Lavrentyev cruise LV29 (Biebow et al., 2003); R/V Sonne cruise SO178, (Dullo and Biebow, 2004); R/V Sonne cruise SO201-2, (Dullo et al., 2009); R/V Akademik M.A. Lavrentyev cruise LV55 (Gorbarenko, 2012); R/V Akademik M.A. Lavrentyev cruise LV63 (Gorbarenko, 2014). Multicore samples for biomarker analysis were sampled in 1 cm thick sections on board and stored under cool and dark conditions in glass bottles or plastic bags (Whirl-Pak™) until further processing. We further include published biomarker data from Multicores recovered from coastal marine sites throughout SE Alaska (16 samples, Prahl et al., 2010) and from R/V Sonne expedition SO202 to the eastern Bering Sea and North Pacific (39 samples, Gersonde et al., 2012; Méheust et al., 2013, Fig. 1). The entire North Pacific dataset consists of 97 Multicore samples summarized in Table 1.

All sample material was freeze-dried and homogenized prior to biomarker analysis. For each lipid analysis, 1–5 g of sediment were extracted with an accelerated solvent extractor (ASE-200, Dionex) at 100 °C and 1000 psi for 15 min by using dichloromethane (DCM) as solvent. Remaining extracts were separated by silica gel column chromatography into three sub-fractions with the following mixture of solvents: fraction 1, 5 ml hexane; fraction 2, a mixture of 5 ml DCM\hexane (1:1); fraction 3, 5 ml DCM. Alkenones were eluted in the third fraction and prepared in 100 µl hexane. In a few cases with lower alkenone abundance, sediment extracts were further concentrated in 20 µl hexane to avoid adsorption effects due to low alkenone concentrations (Grimalt et al., 2001). The third fraction was measured using a HP 6890 gas chromatograph, equipped with a cold injection system, a DB-1MS fused silica capillary column (60 × 0.32 mm inner diameter, film thickness of 0.25 mm) and a flame ionization detector at the Alfred Wegener Institute, Helmholtz Centre for Polar and Marine Research (AWI). Individual alkenone identification ($C_{37:3}$, $C_{37:2}$) was based on the retention time and comparison with an external standard, which were also used for controlling the instrument stability. Replicate analyses of a reference standard suggest an analytical uncertainty of ~0.5 °C for U_{37}^K . The alkenone unsaturation index as proxy for SST

(Prahl and Wakeham, 1987) was determined for all core-top samples. SSTs were calculated using the relationship between U_{37}^K and mean annual temperature ($U_{37}^K = 0.033T + 0.044$) based on global core-top sediments between 60°S and 60°N in the Atlantic, Indian and Pacific oceans (Müller et al., 1998). The standard error of this calibration is reported as ± 0.050 U_{37}^K units or ca. ± 1.5 °C.

4. Results

Results of reconstructed SSTs from sediment surface samples were now compared to instrumental mean annual temperature data. At this point, the choice of the instrumental dataset is critical. For example, instrumental time-series show a strong warming trend in the Bering Sea leading to instrumental mean annual temperatures that are >0.5 °C higher in 2009 compared to 1994 (see also Ren et al., 2014). Our dataset is composed of surface sediment samples collected from 1997 to 2013. To minimize the effect of recent warming in the subpolar Pacific to our dataset we extracted instrumental mean annual temperature data from World Ocean Atlas 2005 (WOA05; Locarnini et al., 2006) using the data analysis and visualization software Ocean Data View (Schlitzer, 2015). The reconstructed temperatures range between 2.7 °C and 18.2 °C in the study area and largely reflect the latitudinal trend in SSTs as expected from WOA05 data (Fig. 2a and b; Table 1).

In a next step, residuals were calculated for each data point by subtracting mean annual SST (WOA05) from respective reconstructed U_{37}^K -based SSTs (Fig. 2c and d; Table 1). Positive residuals of U_{37}^K -based SSTs reflecting warmer than mean annual SST and negative residuals colder than mean annual SST. South of the SAF U_{37}^K -based SSTs show a reasonable fit to mean annual temperatures, and with a few exceptions, residuals do not exceed the reported standard error of calibration of ±1.5 °C (Fig. 2c and d, Table 1). However, a closer look to study sites north of the SAF reveals large discrepancies between instrumental mean annual SST (WOA05) and alkenone temperatures. U_{37}^K -based SSTs overestimate instrumental mean annual temperatures by up to 5.3 °C in the central subpolar Pacific and Gulf of Alaska, up to 3 °C in the Bering Sea and up to even 6.1 °C in the Okhotsk Sea (Fig. 2c and d, Table 1). Warmer than expected reconstructed mean annual SSTs are apparent throughout the entire subpolar Pacific, including the Bering Sea and Okhotsk Sea, thus indicating that reconstructed temperatures north of the SAF generally overestimate instrumental mean annual SST. Only at a few sites located off the coast of East Kamchatka and at northernmost sites of the Bering Sea and Okhotsk Sea, calculated residuals are within the error of the U_{37}^K calibration (Fig. 2c and d).

5. Discussion

Based on our SST compilation we found significant regional discrepancies north and south of the SAF. Alkenone SSTs from core locations south of the SAF largely mimic the mean annual temperature signal (Fig. 2c), which are in accordance with available sediment trap data providing evidence for extended growth season of coccolithophorids from the beginning of spring (March) until autumn (November) in the mid-latitude Northwest Pacific (Yamamoto et al., 2007). Thus, we presume that the better fit of reconstructed SST to instrumental mean annual SST in the mid-latitude Pacific reflects an extended, almost year-round growth season south of the SAF.

Considering the data north of the SAF, a systematic and non-random pattern in departure from core-top alkenone SST versus instrumental mean annual SST is apparent in all different regions of

Table 1

Location, sample depth and data from North Pacific Muticores

Station	Latitude (°N)	Longitude (°E)	Water depth (m)	Sample depth (cm)	U ^K ₃₇	Alkenone temperature (°C)			Residuals (°C)					
						Müller et al. (1998) ^c	Müller et al. (1998) ^d	Sikes et al. (1997) ^e	SSTU ^K ₃₇ (Müller et al., 1998) ^c - WOA05 _{MAT}	SSTU ^K ₃₇ (Müller et al., 1998) ^c - WOA05 _{Autumn (Oct.) SST}	SSTU ^K ₃₇ (Müller et al., 1998) ^d - WOA05 _{Autumn (Oct.) SST}	SSTU ^K ₃₇ (Sikes et al., 1997) ^e - WOA05 _{Autumn (Oct.) SST}		
North Pacific		(north of SAF)												
LV63-28	55.72	163.51	2347	0–1	0.212	5.1	4.3	7.7	0.6	-3.5	-4.4	-0.9		
LV63-33	54.34	162.14	1924	0–1	0.243	6.1	5.3	8.6	0.9	-3.2	-4.0	-0.7		
LV63-41	52.57	160.11	1924	0–1	0.220	5.4	4.5	8.0	0.8	-2.7	-3.5	-0.1		
SO201 -2-11	53.99	162.37	2169	0–1	0.266	6.7	6.0	9.2	1.6	-2.5	-3.2	-0.1		
SO202-01-3 ^a	44.03	152.92	5282	0–1	0.427	11.6	11.2	13.4	3.8	-1.1	-1.5	0.7		
SO202-02-4 ^a	46.97	156.98	4822	0–1	0.333	8.8	8.2	10.9	3.9	0.5	-0.1	2.6		
SO202-03-4 ^a	49.61	160.38	5429	0–1	0.386	10.4	9.9	12.3	5.3	1.9	1.4	3.8		
SO202-04-3 ^a	51.86	163.16	5273	0–1	0.372	9.9	9.4	11.9	4.7	1.4	0.8	3.4		
SO202-05-3 ^a	52.70	164.92	3362	0–1	0.277	7.1	6.4	9.4	1.8	-1.6	-2.3	0.8		
SO202-06-2 ^a	51.90	166.49	3422	0–1	0.358	9.5	9.0	11.6	4.1	1.0	0.4	3.0		
SO202-07-2 ^a	51.27	167.70	2349	0–1	0.317	8.3	7.6	10.5	2.8	-0.2	-0.9	2.0		
SO202-08-1 ^a	50.54	170.82	3630	0–1	0.334	8.8	8.2	10.9	3.1	0.1	-0.4	2.3		
SO202-09-2 ^a	49.66	175.16	5028	0–1	0.407	11.0	10.5	12.9	5.0	2.5	2.0	4.3		
SO202-23-4 ^a	52.17	-160.50	4613	0–1	0.325	8.5	7.9	10.7	1.7	-0.3	-0.9	1.9		
SO202-24-2 ^a	53.00	-157.19	4565	0–1	0.32	8.4	7.7	10.6	1.5	-0.7	-1.3	1.5		
SO202-25-1 ^a	54.10	-152.69	4588	0–1	0.368	9.8	9.3	11.8	2.8	0.9	0.4	3.0		
SO202-26-1 ^a	54.64	-150.38	742	0–1	0.379	10.2	9.6	12.1	3.0	0.9	0.4	2.9		
SO202-27-1 ^a	54.30	-149.60	2916	0–1	0.4	10.8	10.3	12.7	3.6	1.3	0.9	3.2		
SO202-28-1 ^a	54.42	-148.88	3710	0–1	0.372	9.9	9.4	11.9	2.7	0.5	0.0	2.5		
SO202-29-5 ^a	52.03	-148.89	3984	0–1	0.32	8.4	7.7	10.6	0.9	-1.6	-2.3	0.6		
SO202-31-5 ^a	49.68	-152.55	3744	0–1	0.345	9.1	8.5	11.2	1.2	-1.9	-2.5	0.2		
81 ^b	59.94	-143.72	176	0–1	0.37	9.9	9.4	11.9	1.5	0.3	-0.2	2.4		
Bering Sea														
LV63-14	57.22	170.58	1073	0–1	0.220	5.3	4.5	8.0	0.7	-0.6	-1.4	2.0		
LV63-16	61.00	-178.47	171	0–1	0.134	2.7	1.8	5.7	-0.4	-2.6	-3.6	0.3		
SO201-2-76	56.19	170.41	2133	0–1	0.284	7.3	6.6	9.7	2.7	0.9	0.2	3.2		
SO201-2-83	57.30	170.24	970	0–1	0.207	4.9	4.1	7.6	0.6	-1.0	-1.8	1.7		
SO201-2-90	58.71	171.40	1614	0–1	0.232	5.7	4.9	8.3	1.6	0.3	-0.5	2.9		
SO202-10-2 ^a	52.74	179.85	1488	0–1	0.31	8.1	7.4	10.3	2.7	0.7	0.1	3.0		
SO202-11-1 ^a	53.11	178.90	2704	0–1	0.318	8.3	7.7	10.5	3.0	1.0	0.4	3.2		
SO202-12-2 ^a	54.05	179.09	2108	0–1	0.284	7.3	6.6	9.6	2.1	0.1	-0.6	2.5		
SO202-13-4 ^a	54.98	177.96	1383	0–1	0.313	8.2	7.5	10.4	3.0	1.0	0.3	3.2		
SO202-14-5 ^a	56.79	178.82	3822	0–1	0.266	6.7	6.0	9.2	1.8	-0.1	-0.9	2.3		
SO202-15-4 ^a	59.51	-179.85	3137	0–1	0.243	6.0	5.3	8.6	1.8	0.2	-0.5	2.8		
SO202-16-1 ^a	60.40	-179.11	548	0–1	0.213	5.1	4.3	7.8	1.4	-0.2	-1.0	2.5		
SO202-18-1 ^a	60.13	-179.44	1108	0–1	0.256	6.4	5.7	8.9	2.5	0.6	-0.1	3.1		
SO202-19-1 ^a	57.65	-175.68	1751	0–1	0.225	5.5	4.7	8.1	0.9	-0.8	-1.6	1.8		
SO202-21-2 ^a	54.79	-170.33	1911	0–1	0.257	6.5	5.7	8.9	1.0	-0.8	-1.5	1.7		
SO202-22-1 ^a	54.57	-168.81	1478	0–1	0.285	7.3	6.6	9.7	1.6	-0.1	-0.8	2.3		
Okhotsk Sea														
GE99-1-3	45.63	144.34	795	1–3	0.387	10.4	11.0	12.4	3.7	-0.7	-1.2	1.3		
GE99-2-2	46.70	144.79	3040	1–3	0.393	10.6	8.2	12.5	4.1	-0.1	-0.5	1.9		
GE99-4-3	48.03	143.58	75	1–3	0.377	10.1	7.4	12.1	4.4	0.2	-0.3	2.2		
GE99-5-2	47.42	145.38	495	1–3	0.346	9.2	7.9	11.3	3.9	0.0	-0.6	2.1		
GE99-6-3	47.19	148.23	3360	1–3	0.296	7.7	8.6	10.0	3.2	-0.7	-1.4	1.6		
GE99-10-2	48.38	146.17	1390	1–2	0.363	9.7	9.2	11.7	5.2	1.2	0.6	3.2		
GE99-12-3	53.05	144.95	930	0–1	0.297	7.7	9.5	10.0	4.6	-0.3	-1.0	2.0		
GE99-30-2	54.40	145.15	1470	0–1	0.287	7.4	6.3	9.7	4.0	1.1	0.4	3.4		
GE99-31-3	54.47	146.17	1600	1–2	0.206	4.9	7.6	7.6	1.6	-1.9	-2.7	0.8		
GE99-38-3	49.35	150.49	1080	1–3	0.335	8.8	9.6	11.0	4.7	0.8	0.2	3.0		
LV27-3-2	54.42	145.14	1476	2–3	0.276	7.0	9.9	9.4	3.9	0.7	0.0	3.1		

Table 1 (continued)

Station	Latitude (°N)	Longitude (°E)	Water depth (m)	Sample depth (cm)	U ₃₇ ^K	Alkenone temperature (°C)			Residuals (°C)			
						Müller et al. (1998) ^c	Müller et al. (1998) ^d	Sikes et al. (1997) ^e	SSTU ₃₇ ^K (Müller et al., 1998) ^c	SSTU ₃₇ ^K - WOA05 _{MAT}	SSTU ₃₇ ^K (Müller et al., 1998) ^c	SSTU ₃₇ ^K - WOA05 _{Autumn (Oct.) SST}
LV28-2-2	48.55	146.05	1286	1–2	0.359	9.6	10.1	11.6	5.1	1.1	0.5	3.1
LV28-4-3	51.38	145.55	675	0–1	0.324	8.5	9.4	10.7	4.8	-0.5	-1.1	1.7
LV28-40-3	51.36	147.24	1313	0–1	0.374	10.0	7.9	12.0	6.1	0.8	0.3	2.8
LV28-41-3	51.82	149.19	1068	0–1	0.370	9.9	7.5	11.9	5.7	0.6	0.0	2.6
LV28-42-3	51.74	151.18	1036	0–1	0.341	9.0	7.0	11.2	4.8	0.0	-0.6	2.1
LV28-43-3	52.03	152.43	842	0–1	0.323	8.5	6.7	10.7	4.2	-0.6	-1.2	1.6
LV28-61-3	48.26	146.26	1714	0–1	0.360	9.6	8.2	11.6	5.1	1.1	0.5	3.1
LV28-64-3	47.96	146.15	2480	0–2	0.314	8.2	9.0	10.4	3.2	-0.3	-0.9	1.9
LV29-69-1	45.46	144.26	881	1–2	0.419	11.4	7.2	13.2	4.7	0.3	-0.2	2.1
LV29-70-3	48.22	146.27	2165	0–1	0.370	9.9	11.2	11.9	5.4	0.7	0.2	2.7
LV29-94-1	55.09	145.30	1147	1–2	0.269	6.8	9.1	9.2	4.0	1.1	0.3	3.5
LV29-104-1	53.46	146.29	1752	1–2	0.333	8.8	7.6	10.9	5.3	0.6	0.0	2.7
LV29-106-1	52.01	154.04	515	0–0.5	0.303	7.9	8.4	10.1	3.5	-1.0	-1.7	1.3
LV29-108-3	52.05	153.83	625	1–2	0.314	8.2	4.1	10.4	3.8	-0.7	-1.3	1.5
LV29-110-1	50.50	155.01	1218	0–1	0.309	8.0	9.4	10.3	4.1	0.1	-0.6	2.3
LV29-112-1	50.36	154.40	1306	1–2	0.270	6.9	6.2	9.3	3.0	-0.7	-1.4	1.7
LV29-114-1	49.54	152.92	1789	1–2	0.311	8.1	6.8	10.3	4.1	0.6	0.0	2.9
LV29-131-1	45.74	144.38	760	0–1	0.426	11.6	6.1	13.4	4.9	0.5	0.1	2.3
LV55-9	49.50	153.46	1993	0–1	0.289	7.4	7.0	9.8	3.2	0.0	-0.7	2.3
LV55-12	53.33	152.30	728	0–1	0.302	7.8	6.8	10.1	3.7	-1.0	-1.7	1.3
LV55-18	56.34	145.31	307	0–1	0.224	5.5	7.2	8.1	2.0	1.5	0.7	4.1
SO178-37-1	54.51	144.29	871	1–2	0.291	7.5	4.7	9.8	4.5	1.2	0.5	3.5
North Pacific (south of SAF)												
SO202-32-5 ^a	45.50	-158.50	5302	0–1	0.369	9.8	9.3	11.9	0.3	-3.6	-3.0	-1.6
SO202-33-5 ^a	45.08	-174.14	6159	0–1	0.383	10.3	9.8	12.2	1.0	-2.1	-1.1	-0.1
SO202-34-2 ^a	40.89	-177.68	5713	0–1	0.507	14.0	13.8	15.5	0.5	-4.3	-2.1	-2.8
SO202-36-6 ^a	38.19	176.70	4522	0–1	0.565	15.8	15.6	17.0	0.1	-4.8	-2.8	-3.6
SO202-37-1 ^a	37.77	176.27	3573	0–1	0.584	16.4	16.3	17.5	-0.4	-4.3	-3.4	-3.1
SO202-38-1 ^a	38.04	169.28	5503	0–1	0.573	16.0	15.9	17.2	0.1	-4.5	-3.6	-3.3
SO202-39-2 ^a	38.01	164.45	5096	0–1	0.617	17.4	17.3	18.4	0.3	-3.3	-3.5	-2.2
SO202-40-2 ^a	38.00	162.68	3462	0–1	0.566	15.8	15.7	17.1	0.0	-4.9	-5.5	-3.7
SO202-41-3 ^a	38.41	160.33	5408	0–1	0.643	18.2	18.2	19.1	2.3	-2.7	-2.0	-1.8
SO202-42-3 ^a	38.89	157.63	5535	0–1	0.641	18.1	18.1	19.0	2.1	-2.8	-2.0	-1.9
SO202-45-2 ^a	40.29	149.49	5476	0–1	0.547	15.2	15.1	16.6	2.6	-3.9	-1.9	-2.6
3 ^b	54.81	-133.27	193	0–1	0.302	7.8	7.2	10.1	-1.7	-5.2	-4.1	-2.9
6 ^b	54.96	132.74	400	0–1	0.38	10.2	9.7	12.2	0.7	-2.8	-1.6	-0.9
15 ^b	55.58	-134.67	268	0–1	0.341	9.0	8.4	11.1	-0.1	-3.8	-2.5	-1.7
10 ^b	55.60	-133.49	200	0–1	0.392	10.5	10.1	12.5	1.4	-2.3	-0.8	-0.3
19 ^b	56.77	-135.13	106	0–1	0.313	8.2	7.5	10.4	-1.0	-5.0	-3.4	-2.8
25 ^b	56.79	-136.15	1820	0–1	0.388	10.4	9.9	12.4	1.3	-2.8	-1.0	-0.8
43 ^b	56.96	-135.26	89	0–1	0.303	7.8	7.2	10.1	-1.3	-5.3	-3.7	-3.0
39 ^b	57.00	-135.49	205	0–1	0.337	8.9	8.3	11.0	-0.2	-4.3	-2.6	-2.2
36 ^b	57.10	-135.52	178	0–1	0.3	7.8	7.1	10.1	-1.4	-5.4	-3.8	-3.1
32 ^b	57.15	-135.36	151	0–1	0.347	9.2	8.6	11.3	0.1	-4.0	-2.3	-1.9
29 ^b	57.18	-135.41	119	0–1	0.314	8.2	7.5	10.4	-0.9	-5.0	-3.4	-2.8
46 ^b	57.59	-136.08	178	0–1	0.325	8.5	7.9	10.7	-0.7	-4.8	-3.0	-2.6
65 ^b	57.86	-137.07	430	0–1	0.411	11.1	10.7	13.0	2.0	-2.2	-0.2	-0.3
49 ^b	58.11	-136.47	260	0–1	0.348	9.2	8.6	11.3	0.0	-4.1	-2.3	-2.0
56 ^b	58.13	-134.92	608	0–1	0.376	10.1	9.5	12.1	0.9	-3.2	-1.4	-1.2

^a Data obtained from Méheust et al. (2013).^b Data obtained from Prahl et al. (2010).^c Global core-top calibration; 60°N–60°S (Müller et al., 1998).^d South Atlantic core-top calibrations; Autumn (Müller et al., 1998).^e Southern Ocean, Summer (Sikes et al., 1997).

the subpolar Pacific (Fig. 2c and d). Our study corroborates the reported warm bias between U_{37}^K -based SSTs and mean annual SSTs in coastal marine sites throughout SE Alaska and the subpolar Northeast Pacific (Prahl et al., 2010; Méheust et al., 2013). Based on our extended North Pacific dataset (now including the subpolar Northwest Pacific, western Bering Sea and the Okhotsk Sea), alkenone-based SST estimates from the whole subpolar Pacific Ocean are generally in conflict with the premise from the global core-top calibration of U_{37}^K , where the best fit is obtained with mean annual SST (Müller et al., 1998) (Fig. 2c and d).

5.1. Seasonality and its imprint on sedimentary U_{37}^K -signal north of the SAF: the subpolar Pacific

In the subpolar Pacific marine productivity and export flux patterns to the ocean interior are intimately linked to seasonal variations in meteorological and physical oceanographic conditions (e.g. Honda et al., 2002). From a biological perspective, sedimentary alkenone compositions should reflect the season when productivity of alkenones and flux of this biomarker signal to the sediments appear (e.g. Sikes et al., 1997). The best approach to evaluate the issue of seasonality in alkenone flux possibly encoded in sedimentary U_{37}^K signals is through combination of sedimentary alkenone temperature estimates with modern alkenones flux data derived from sediment trap time series.

In this regard, the North Pacific (including the Okhotsk and Bering Sea) is highly suitable because this region has been thoroughly studied with sediment trap time series during the past decades and seasonal production and export flux of alkenones are relatively well known. To further examine this issue we considered available information from published sediment trap time series of the subpolar Pacific, Bering Sea and Okhotsk Sea to identify times of

alkenone flux to the sediment in the study area (Harada et al., 2003, 2006a; Seki et al., 2007) (Fig. 3a). In the subpolar Northwest Pacific blooms of *E. huxleyi* typically occur from late summer to autumn with maximum flux of alkenones observed during October–November (Harada et al., 2006a). In the Bering Sea and Okhotsk Sea *E. huxleyi* blooms are restricted to the autumn season (September–November), suggesting that alkenones are synthesized during limited periods (Harada et al., 2003; Seki et al., 2007). A more recent study on nineteen-year time-series of coccolithophore fluxes further demonstrates that the main blooming season and export of *E. huxleyi* is heavily biased to October–November in the Bering Sea and subpolar Pacific (Tsutsui et al., 2016). From available sediment trap time series we identified October (autumn) as common midpoint for maximum alkenone flux north of the SAF. Accordingly, we extract respective instrumental October (autumn) SST data from WOA05 that were now compared to sedimentary U_{37}^K -based SSTs (Fig. 3).

Because of strong seasonality in the subpolar Pacific we first took into account the calibration of U_{37}^K ($U_{37}^K = 0.038T - 0.082$) proposed by Sikes et al. (1997) originally obtained from core-top sediments of Southern Ocean. It has been proposed that these calibration better capture seasonally biased SSTs also in the subpolar Pacific (e.g. Méheust et al., 2013). Consequently, U_{37}^K were converted to SSTs according to the Sikes et al. (1997) calibration and results compared to instrumental autumn SST data from WOA05, considering production and export of alkenones to the sediments reported from sediment trap data of the subpolar Pacific. Residuals were calculated for each data point by subtracting autumn SST (WOA05) from respective U_{37}^K -based SSTs applying the Sikes et al. (1997) calibration (Fig. 3c and d; Table 1).

Using the Sikes et al. (1997) calibration, subpolar Pacific, as well as Bering Sea and Okhotsk Sea SST estimates are in general 2–4 °C

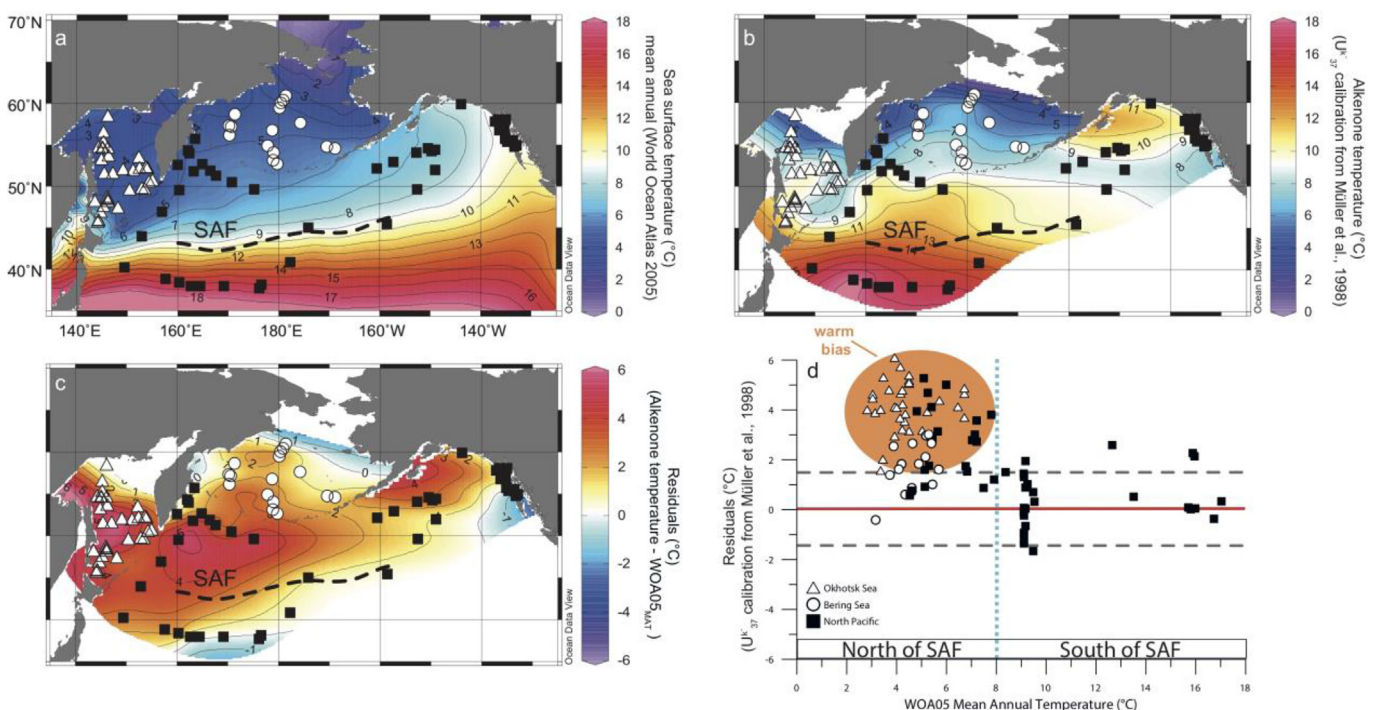


Fig. 2. (a): Distribution of North Pacific Multicore surface samples (symbols) together with gridded mean annual temperature (WOA05; Locarnini et al., 2006). (b): gridded SST data from Multicore surface samples using the global calibration of U_{37}^K (Müller et al., 1998). (c): spatial distribution of residuals (reconstructed SSTs – WOA05_{MAT}). (d): detailed comparison of calculated residuals (reconstructed SSTs – WOA05_{MAT}) north and south of the Subarctic Front (SAF). Dashed lines in gray denote uncertainty of $\pm 1.5^{\circ}\text{C}$ reported for the global calibration of U_{37}^K (Müller et al., 1998). This figure was generated with Ocean Data View (Schlitzer, 2015).

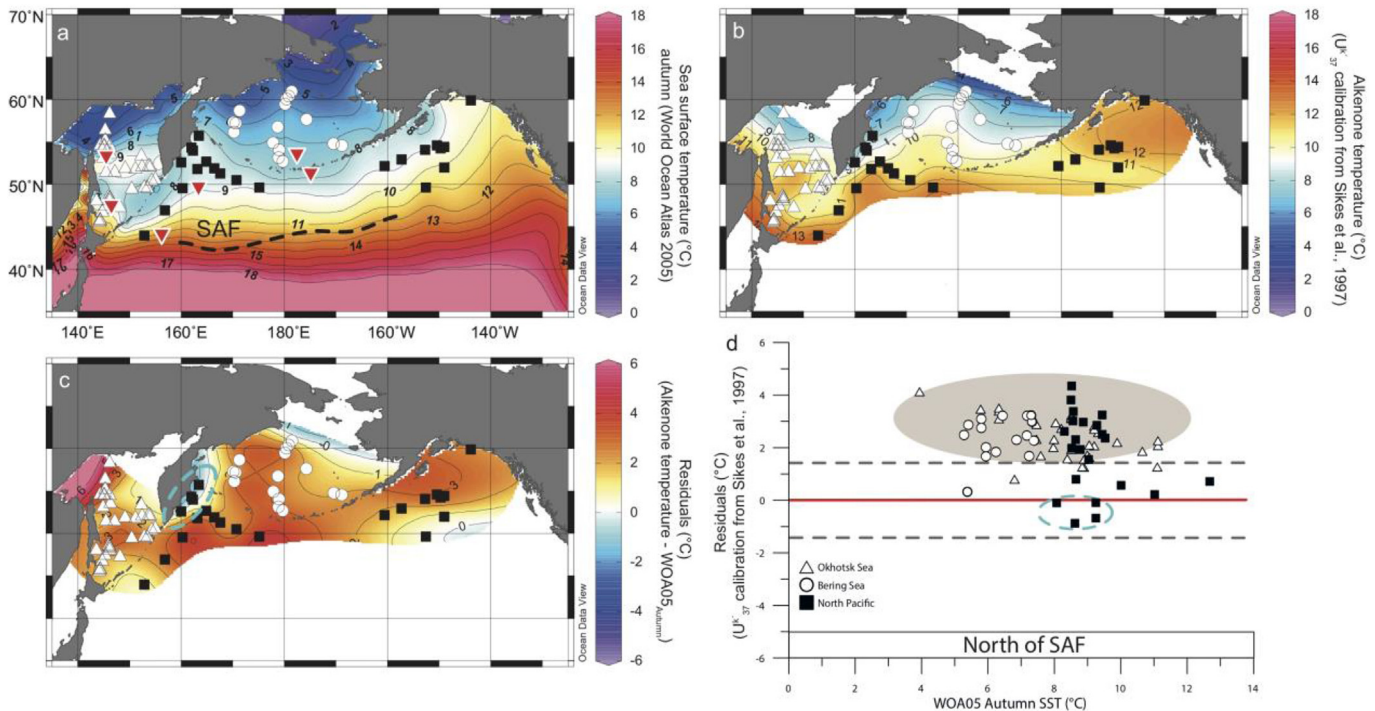


Fig. 3. (a): North Pacific gridded instrumental SSTs (autumn) from WOA05 (Locarnini et al., 2006), with location of Multicore surface samples north of the SAF (symbols). Red triangles mark the sediment trap data location (Harada et al., 2003, 2006a; Seki et al., 2007; Tsutsui et al., 2016) considered in this study. (b): gridded SST data based on seasonal U_{37}^K calibration reported for cold regions (Sikes et al., 1997). (c): spatial distribution of calculated residuals (reconstructed SST_{Sikes et al., 1997} - WOA05_{Autumn}). (d): detailed comparison of calculated residuals (reconstructed SST_{Sikes et al., 1997} - WOA05_{Autumn}) north of the Subarctic Front (SAF). Dashed lines in gray denote uncertainty of $\pm 1.5 ^{\circ}$ C reported for the global calibration of U_{37}^K (Müller et al., 1998). This figure was generated with Ocean Data View (Schlitzer, 2015). (For interpretation of the references to colour in this figure legend, the reader is referred to the Web version of this article.)

warmer than recorded from WOA05 autumn instrumental SST (Fig. 3). Anomalously colder than predicted SST estimates, however, are observed at a few coastal sites near Kamchatka. In general, calculated residuals suggest that the Sikes et al. (1997) calibration in the study area largely overestimates instrumental autumn SSTs (warm bias), as evidenced by very positive residuals of $\sim 2\text{--}4 ^{\circ}$ C. (Fig. 3c and d). We note that results are different to a previous study from Méheust et al. (2013) that proposed a better fit of reconstructed SSTs of the subpolar Pacific using the Sikes et al. (1997) Southern Ocean calibration of U_{37}^K . However, the study of Méheust et al. (2013) did not consider observational data from sediment traps that clearly show the modern blooming period of *E. huxleyi* is heavily biased to the autumn season (Harada et al., 2003; Seki et al., 2007; Tsutsui et al., 2016).

To further evaluate the potential seasonal bias in sedimentary alkenone temperature estimates the commonly used U_{37}^K global core-top calibration equation (Müller et al., 1998) are compared to instrumental autumn SST (Table 1). We note that the U_{37}^K global core-top calibration equation is virtually identical to the initial U_{37}^K calibration based on laboratory culture studies based on North Pacific strain of *E. huxleyi* (Prahl and Wakeham, 1987; Prahl et al., 1988). However, the U_{37}^K global core-top calibration equation is based on sedimentary U_{37}^K , and does better represent natural oceanic conditions and variability. So we move on with the Müller et al. (1998) calibration to compare sedimentary alkenone temperatures to instrumental autumn SST (Fig. 4). Observations from re-examination of SST estimates are surprisingly straightforward. Using the Müller et al. (1998) calibration results in much improved fit between reconstructed SSTs and instrumental autumn SST (Fig. 4). Calculated residuals suggest no significant offset (no warm

bias) within the different regions of the subpolar Pacific. Most study sites are within the standard deviation of $\pm 1.5 ^{\circ}$ C reported for the given calibration (Fig. 4 c and d). Our study thus further corroborates the observation that using the global core-top calibration, would produce errors at the level of $\pm 1.5 ^{\circ}$ C or less, which are not larger than the mean standard error of the entire regression for the global ocean calibration (Herbert, 2003). A bit surprising, further consideration of a seasonal (autumn) calibration of U_{37}^K from Müller et al. (1998) results in a worse fit to instrumental SST in our study area (Table 1, not shown). We conclude that the commonly used calibrations of U_{37}^K of Müller et al. (1998) and Prahl et al. (1988), when seasonality in alkenone production and export are known and considered, are the best estimators (with a few exceptions) of SSTs in the subpolar Pacific (Table 1; Fig. 4d).

Exceptions are again observed at a few sites near the coast off Kamchatka and at the northernmost site in the Bering Sea, where residuals clearly exceed the standard deviation of $\pm 1.5 ^{\circ}$ C (Fig. 4c and d). The northernmost site in the Bering Sea shows anomalously low U_{37}^K -value of 0.135 or $+2.7 ^{\circ}$ C. However, this value is at the lower limit of the temperature range of the global core-top calibration and should not be interpreted quantitatively (e.g. Herbert, 2003). We also observe colder than expected SSTs near the continental margin of Kamchatka that are situated within the outflow region of the EKC (Fig. 4d). We speculate that the anomalous colder than expected U_{37}^K -signal is probably affected by lateral transport of allochthonous alkenones from the Bering Sea to the North Pacific via the EKC. Lateral advection of allochthonous alkenones may obscure U_{37}^K values and has been reported to occur at analogue locations in the North Atlantic proximate to major fronts in SST and nutrients (Rosell-Melé et al., 2000).

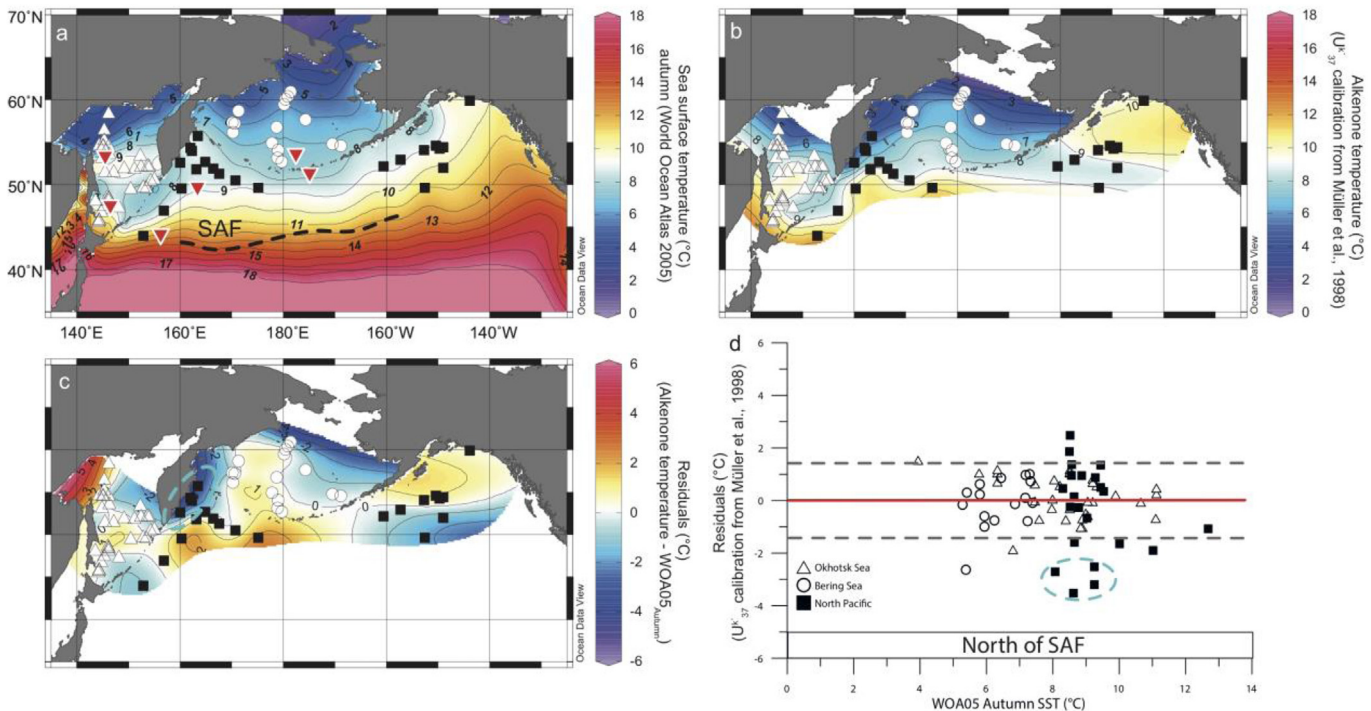


Fig. 4. (a): North Pacific gridded instrumental SSTs (autumn) from WOA05 (Locarnini et al., 2006) together with location of Multicore surface samples north of the SAF (symbols). Red triangles mark the location of sediment trap data (Harada et al., 2003, 2006a; Seki et al., 2007; Tsutsui et al., 2016) that has been considered in this study. (b): gridded SST data based on global U^{37} calibration (Müller et al., 1998). (c): spatial distribution of calculated residuals (reconstructed SST_{Müller et al., 1998} - WOA05_{Autumn}). (d): detailed comparison of calculated residuals (reconstructed SST_{Müller et al., 1998} - WOA05_{Autumn}) north of the Subarctic Front (SAF). Dashed lines in gray denote uncertainty of $\pm 1.5 ^{\circ}\text{C}$ reported for the global calibration of U^{37} (Müller et al., 1998). This figure was generated with Ocean Data View (Schlitzer, 2015). (For interpretation of the references to colour in this figure legend, the reader is referred to the Web version of this article.)

5.2. Potential implications for alkenone-derived SST reconstructions in the subpolar Pacific: a case study from a stratigraphic alkenone record of the Okhotsk Sea

For the subpolar Pacific we demonstrate that the modern U^{37} -signal is tightly coupled to seasonality in alkenone production that needs to be considered to derive meaningful SST estimates from alkenone temperatures. In terms of paleoceanographic reconstructions, very little is known about e.g. seasonality in alkenone production in the geological past. Hence, the basic assumption is that seasonality in alkenone production (if considered at all) did not change e.g. through different climatic intervals. However, the growth season in high-latitude ocean settings might have changed through time, an issue that potentially leads to biased paleoclimatic information drawn from stratigraphic U^{37} -records.

Here, we conduct a case study using an IMAGES sediment core collected from near Hokkaido, in the south-western Okhotsk Sea (Fig. 5a; MD01-2412; lat $44^{\circ}31.65'\text{N}$, long $145^{\circ}00.25'\text{E}$; water depth, 1225 m) to assess a bit further the potential effect of changing growth seasons of coccolithophorides on stratigraphic U^{37} -records. We decided to consider MD01-2412 because it is the only alkenone temperature record from the subpolar Pacific covering the last glacial interval with millennial to centennial temporal resolution. Low alkenone content in MD01-2412 during the LGM has been attributed to enhanced seasonal sea-ice coverage resulting in light limitation on marine productivity and shortened coccolithophorid growth period (Ternois et al., 2000; Harada et al., 2004). Anomalously warm alkenone temperatures were reported from the stratigraphic U^{37} -record of MD01-2412 during the glacial period (Fig. 5). It has been speculated that a shift of the bloom

season of the alkenone producer from autumn to summer may have caused the high alkenone temperatures recorded in the glacial sediments of the south-western Okhotsk Sea (Harada et al., 2006b, 2008).

First, we have a look into the modern seasonal variation in SST at Site MD01-2412 (Fig. 5b). The measured alkenone temperature at the core top is $9.1 ^{\circ}\text{C}$, which is very close to instrumental temperatures in the upper 20 m of the water column during July–August and October–November (Harada et al., 2006b). In the Okhotsk Sea, autumn is the main season of production for *E. huxleyi* and main export of coccospores is from November–December (Broerse et al., 2000; Seki et al., 2007). Thus, modern alkenone temperatures at this study site reflect the autumn SST in the upper 20 m of the water column in autumn (Fig. 5b). Whether a shift of the bloom season to summer (July) may have caused the high alkenone temperatures recorded in the glacial sediments of the south-western Okhotsk Sea (e.g. Harada et al., 2008) we need to estimate the seasonal SST gradient (ΔT). Because seasonal data is not available for the glacial interval we can only consider the modern monthly average data at 20 m water depth from WOA to assess ΔT . Based on instrumental SST data the modern ΔT is $\sim 4.5 ^{\circ}\text{C}$ from summer (July) to autumn (October) season (Fig. 5b) near site MD01-2412. Hence, estimated ΔT is used to mimic a “shifted bloom season” of the alkenone producer from autumn to summer from alkenone time-series for the glacial interval (11–115 ka BP) of MD01-2412.

Comparison of the original alkenone time-series from MD01-2412 (Harada et al., 2006b) and the alkenone time-series with “shifted bloom season” are given in Fig. 5c. Looking at the “shifted bloom season” alkenone time-series the anomalously warm glacial alkenone temperatures have been vanished from the stratigraphic

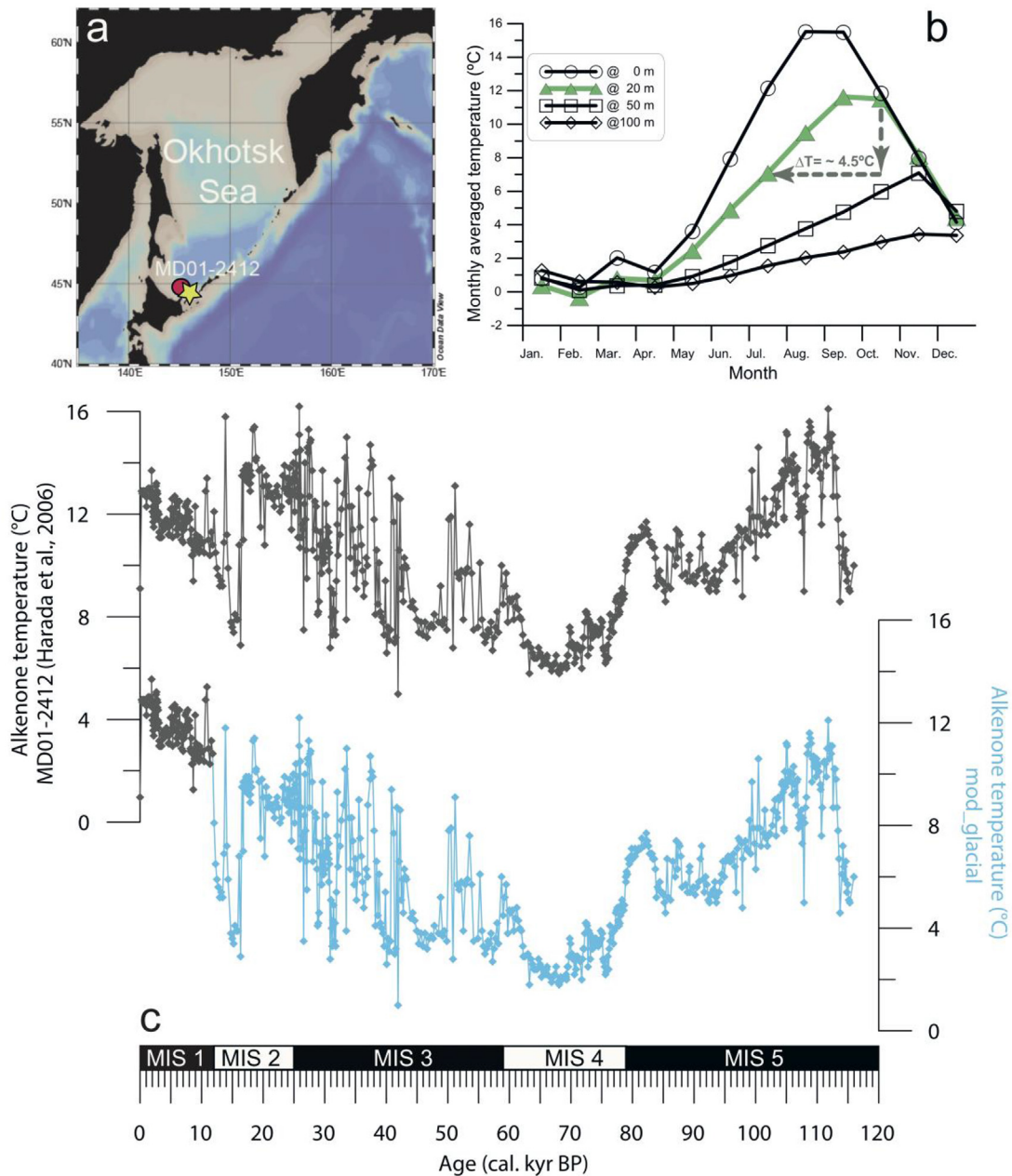


Fig. 5. Case study on seasonality using glacial alkenone time-series of IMAGES core MD01-2412 from the southwestern Okhotsk Sea. (a): Location of MD01-2412 (red spot) and station data from WOA (yellow star). (b): Modern monthly average SST data from WOA05 (Locarnini et al., 2006) (c): Comparison of original MD01-2412 alkenone time-series (in gray; Harada et al., 2006b) and the alkenone time-series with glacial "shifted bloom season" (in blue; this study). (For interpretation of the references to colour in this figure legend, the reader is referred to the Web version of this article.)

U_{37}^K -record. Based on this exercise, glacial alkenone temperatures at Site MD01-2412 are now about $\sim 2.5^\circ\text{C}$ colder than during the Holocene. Hence, a past shift of the bloom season of the alkenone producer at Site MD01-2412 may explain a large part of anomalously high alkenone temperatures recorded in the glacial sediments of the south-western Okhotsk Sea (Harada et al., 2006b). Considering a glacial shift of the main production season of alkenones the time-series now better fits to available TEX_{86} biomarker reconstructions and numerical simulations that also show colder glacial than Holocene SST of the central Okhotsk Sea during the glacial period (Lo et al., 2018). Lower glacial than Holocene SSTs have been also reported from TEX_{86} biomarker reconstructions of the Bering Sea and the subpolar Northwest Pacific (Meyer et al.,

2017). However, results of this case study are based on modern monthly average data from WOA. Hence, doubts are allowed how meaningful these results for paleoclimatic reconstructions really are. Nevertheless, our case study from the Okhotsk Sea underpins the potentially important role of seasonality on high-latitude settings with even small shifts in past bloom seasons may lead to heavily biased SST information drawn from such stratigraphic U_{37}^K -records.

5.3. Further implications

Based on combination of modern alkenone flux data from sediment trap time series with a comprehensive dataset of

$\text{U}_{37}^{\text{K'}}$ -based SSTs from North Pacific core-tops revealed that $\text{U}_{37}^{\text{K'}}$ -based SST estimates largely correspond to instrumental SSTs during times of maximum export flux of alkenones in the subpolar Pacific. These results are in line with former observations from subantarctic waters where alkenone-based SST reproduces the SST values when alkenone flux to the sediment high (e.g. Sikes et al., 2005). It reinforces the idea that $\text{U}_{37}^{\text{K'}}$, when seasonality in alkenone production and export are known and considered, is able to provide reasonable estimates of SSTs in high-latitude ocean settings (e.g. Prah� et al., 2010) and further attest, in principle, to the validity for wide use of the original global core-top calibration equation by Müller et al. (1998) to estimate past SSTs.

Given above considerations, our conclusions differ from studies that have tried to re-define the global core-top calibration to account for a seasonal bias in alkenones (Conte et al., 2006; Tierney et al., 2018). It has been shown that in case of subpolar oceans, the resultant nonlinear calibrations do not reduce the uncertainty in SST substantially (Tierney et al., 2018). According to our results, residuals in the lower temperature range of the linear global calibration equation for $\text{U}_{37}^{\text{K'}}$ are not entirely random, but hold valuable information about secondary controls encoded in the sedimentary $\text{U}_{37}^{\text{K'}}$ -signal, such as seasonality in production and export of alkenones in the subpolar Pacific. Finally, seasonality of maximum alkenone flux in sediment traps varies across the oceans and through time, a consistent, globally applicable, seasonal pattern is still not apparent (Rosell-Melé and Prah�, 2013). Further studies combining sediment trap time series with sedimentary $\text{U}_{37}^{\text{K'}}$ -records are the key to identify regional differences in the $\text{U}_{37}^{\text{K'}}$ -signal in marine surface sediments and to further improve paleoceanographic interpretations based on sedimentary alkenone records.

6. Conclusions

In this study, we present a compilation of 97 sediment surface samples from Multicores collected in the Bering Sea, the Okhotsk Sea and the North Pacific that has been used to evaluate the alkenone-temperature proxy against observational data in the high-latitudes of the North Pacific. Surface samples were analysed for alkenones and the $\text{U}_{37}^{\text{K'}}$ -index converted to water temperatures using different calibration equations established in the literature. We found that south of the SAF alkenone derived SSTs show a reasonable fit to mean annual temperatures. However, study sites north of the SAF do not match instrumental mean annual SST and alkenone temperatures show a large, systematic offset (warm bias) throughout all different regions of the subpolar Pacific. To further investigate this issue we combined information from instrumental SST data as well as modern alkenone flux data from sediment traps to investigate the role of seasonality on the sedimentary alkenone-signal. Comparison of the sedimentary alkenone-signal to observational data revealed that $\text{U}_{37}^{\text{K'}}$ -based SSTs match modern autumn temperatures north of the Subarctic Front (SAF), when maximum export flux of alkenones to the seafloor is indicated by sediment trap data. Most sample sites are within the standard deviation of $\pm 1.5^{\circ}\text{C}$ reported for the global calibration provided by Müller et al. (1998). Our results demonstrate that $\text{U}_{37}^{\text{K'}}$, when seasonality in alkenone production and export are known and considered, is a robust proxy for SSTs in high-latitude ocean settings. We conduct a case study using an IMAGES sediment core collected from the south-western Okhotsk Sea to assess the potential effect of seasonality on stratigraphic $\text{U}_{37}^{\text{K'}}$ -records in the subpolar Pacific. The case study from the Okhotsk Sea show that even a small shift in

seasonality may lead to strongly biased SST reconstructions with broader implications for paleoclimatic information drawn from such stratigraphic $\text{U}_{37}^{\text{K'}}$ -records.

Author statement

L.M., L.L.-J., X.S., and R.T. designed research; L.M., and J.Z. performed research; L.M. analysed data; and L.M., J.Z., and L.L.-J. wrote the paper.

Declaration of competing interest

The authors declare that they have no known competing financial interests or personal relationships that could have appeared to influence the work reported in this paper.

Acknowledgements

We gratefully acknowledge the professional support of Masters and Crews during R/V Marshal Gelovany, R/V Akademik Lavrentiev and R/V Sonne expeditions GE99, LV27, LV28, LV29, LV55, LV63, SO178 and SO201-2 to the Okhotsk Sea, Bering Sea and North Pacific from 1997 to 2013. We express our thanks to K. Fahl and W. Luttmer for analytical assistance with biomarker measurements at the Alfred Wegener Institute Helmholtz Centre for Polar and Marine Research. We acknowledge funding by the Bundesministerium für Bildung und Forschung (BMBF) through grants 03F0704A (SIGEPAX) and 03F0785A (NOPAWAC), the Helmholtz Climate Initiative REKLIM (Regional climate change), the National Program on Global Change and Air-Sea Interaction (GASI-GEOGE-04), the National Natural Science Foundation of China (Grant Nos.: 41476056, U1606401), and the AWI research programme PACES II. Supplementary data are available via PANGAEA Data Publisher for Earth and Environmental Science (<https://doi.org/10.1594/PANGAEA.920779>).

References

- Bard, E., Rostek, F., Sonzogni, C., 1997. Interhemispheric synchrony of the last deglaciation inferred from alkenone palaeothermometry. *Nature* 385, 707–710.
- Bard, E., Rostek, F., Turon, J.L., Gendreau, S., 2000. Hydrological impact of Heinrich events in the subtropical northeast Atlantic. *Science* 289, 1321–1324.
- Bauch, H.A., Kandiano, E.S., Helmke, J., Andersen, N., Rosell-Melé, A., Erlenkeuser, H., 2011. Climatic bisection of the last interglacial warm period in the Polar North Atlantic. *Quat. Sci. Rev.* 30, 1813–1818.
- Biebow, N., Hüttner, E., 1999. KOMEX (kurile Okhotsk Sea marine experiment) cruise reports: KOMEX I and II, RV professor gagarinsky cruise 22, RV Akademik M.A. Lavrentiev cruise 28. In: GEOMAR Report 82, Kiel, Germany, p. 188.
- Biebow, N., Lüdmann, T., Karp, B.Y., Kulich, R., 2000. KOMEX (Kurile Okhostk Sea Marine Experiment) RV Professor Gagarinsky Cruise 26, vol. 1. MV Marshal Gelovany Cruise, Kiel, Germany, p. 296. GEOMAR Report 88.
- Biebow, N., Kulich, R., Baranov, B., 2003. KOMEX II, kurile Okhotsk Sea marine experiment: cruise report RV Akademik M.A. Lavrentev cruise 29. Leg1 and Leg 2. GEOMAR Report, 110, Kiel, Germany, p. 190.
- Brassell, S.C., Eglington, G., Marlowe, I.T., Pflaumann, U., Sarnthein, M., 1986. Molecular stratigraphy – a new tool for climatic assessment. *Nature* 320, 129–133.
- Broerse, A.T.C., Ziveri, P., Honjo, S., 2000. Coccolithophore (-CaCO₃) flux in the Sea of Okhotsk: seasonality, settling and alteration processes. *Mar. Micropaleontol.* 39, 179–200.
- Conte, M.H., Thompson, A., Lesley, D., Harris, R.P., 1998. Genetic and physiological influences on the alkenone/alkenoate versus growth temperature relationship in *Emiliania huxleyi* and *Gephyrocapsa oceanica*. *Geochem. Cosmochim. Acta* 62, 51–68.
- Conte, M.H., Sicre, M.A., Ruhemann, C., Weber, J.C., Schulte, S., Schulz-Bull, D., Blanz, T., 2006. Global temperature calibration of the alkenone unsaturation index UK'37 in surface waters and comparison with surface sediments. *G-cubed* 7, 1–22.
- Dullo, W.C., Biebow, N., 2004. SO178-KOMEX Cruise Report: Mass Exchange Processes and Balances in the Okhotsk Sea. IFM-GEOMAR Report, Kiel, Germany, p. 125.
- Dullo, W.C., Baranov, B., van den Bogaard, C., 2009. FS Sonne Fahrbericht/Cruise Report SO201-2 KALMAR, Busan/Korea-Tomakomai/Japan, 30.08-08.10.2009, p. 233. IFM-GEOMAR Report 35, Kiel, Germany.

- Epstein, B.L., D'Hondt, S., Quinn, J.G., Zhang, J.P., Hargraves, P.E., 1998. An effect of dissolved nutrient concentrations on alkenone-based temperature estimates. *Paleoceanography* 13, 122–126.
- Gersonde, R., 2012. The Expedition of the Research Vessel "Sonne" to the Subpolar North Pacific and the Bering Sea in 2009 (SO202-INOPEX), vol. 643. Reports on Polar and Marine Research, Bremerhaven, Germany, p. 323.
- Gong, C., Hollander, D.J., 1999. Evidence for differential degradation of alkenones under contrasting bottom water oxygen conditions: implication for paleotemperature reconstruction. *Geochem. Cosmochim. Acta* 63, 405–411.
- Gorbarenko, S., 2012. R/V Academician M.A.lavrentyev cruise 55 sea of Okhotsk, p. 78, 7 July – 6 August, 2011, Cruise Report.
- Gorbarenko, S., 2014. R/V Academician M.A.lavrentyev Cruise 63 Bering Sea and the Northwestern Pacific, 21 July - 03 September, 2013, Cruise Report, p. 177.
- Grimalt, J.O., Calvo, E., Pelejero, C., 2001. Sea surface paleotemperature errors in UK'37 estimation due to alkenone measurements near the limit of detection. *Paleoceanography* 16, 226–232.
- Harada, N., Shin, K.H., Murata, A., Uchida, M., Nakatani, T., 2003. Characteristics of alkenones synthesized by a bloom of *Emiliania huxleyi* in the Bering Sea. *Geochem. Cosmochim. Acta* 67, 1507–1519.
- Harada, N., Ahagon, N., Uchida, U., Murayama, M., 2004. Northward and southward migrations of frontal zones during the past 40 kyr in the Kuroshio-Oyashio transition area. G-cubed 5, Q09004. <https://doi.org/10.1029/2004GC000740>.
- Harada, N., Sato, M., Shiraishi, A., Honda, M.C., 2006a. Characteristics of alkenone distributions in suspended and sinking particles in the northwestern North Pacific. *Geochem. Cosmochim. Acta* 70, 2045–2062.
- Harada, N., Ahagon, N., Sakamoto, T., Uchida, M., Ikehara, M., Shibata, Y., 2006b. Rapid fluctuation of alkenone temperature in the southwestern Okhotsk Sea during the past 120 kyr. *Global Planet. Change* 53, 29–46.
- Harada, N., Sato, M., Sakamoto, T., 2008. Freshwater impacts recorded in tetraunsaturated alkenones and alkenone sea surface temperatures from the Okhotsk Sea across millennial-scale cycles. *Paleoceanography* 23 (3), PA3201. <https://doi.org/10.1029/2006PA001410>.
- Harada, N., Katsuki, K., Nakagawa, M., Matsumoto, A., Seki, O., Addison, J.A., Finney, B.P., Sato, M., 2014. Holocene sea surface temperature and sea ice extent in the Okhotsk and Bering Seas. *Prog. Oceanogr.* 126, 242–253.
- Herbert, T.D., 2003. Alkenones as paleotemperature indicators. In: Turekian, K.K., Holland, H.D. (Eds.), *Treatise on Geochemistry*. Elsevier Science, pp. 391–432.
- Herbert, T.D., Peterson, L.C., Lawrence, K.T., Liu, Z.H., 2010. Tropical ocean temperatures over the past 3.5 million years. *Science* 328, 1530–1534.
- Ho, S.L., Mollenhauer, G., Lamy, F., Martinez-Garcia, A., Mohtadi, M., Gersonde, R., Hebbeln, D., Nunez-Ricardo, S., Rosell-Mele, A., Tiedemann, R., 2012. Sea surface temperature variability in the Pacific sector of the Southern Ocean over the past 700 kyr. *Paleoceanography* 27, PA4202.
- Hoebs, M.J.L., Versteegh, G.J.M., Rijpstra, W.I.C., de Leeuw, J.W., Damste, J.S.S., 1998. Postdepositional oxic degradation of alkenones: implications for the measurement of palaeo sea surface temperatures. *Paleoceanography* 13, 42–49.
- Honda, M.C., Imai, K., Nojiri, Y., Hoshi, F., Sugawara, T., Kusakabe, M., 2002. The biological pump in the northwestern North Pacific based on fluxes and major components of particulate matter obtained by sediment-trap experiments (1997–2000). Deep-Sea Reserach Part II-Topical Studies in Oceanography 49, 5595–5625.
- Ikehara, M., Kawamura, K., Ohkouchi, N., Kimoto, K., Murayama, M., Nakamura, T., Oba, T., Taira, A., 1997. Alkenone sea surface temperature in the Southern Ocean for the last two deglaciations. *Geophys. Res. Lett.* 24, 679–682.
- Lo, L., Belz, S.T., Lattaud, J., Friedrich, T., Zeeden, C., Schouten, S., Smik, L., Timmermann, A., Cabedo-Sanz, P., Huang, J.J., Zhou, L., Ou, T.H., Chang, Y.P., Wang, L.C., Chou, Y.M., Shen, C.C., Chen, M.T., Wei, K.Y., Song, S.R., Fang, T.H., Gorbarenko, S.A., Wang, W.L., Lee, T.Q., Elderfield, H., Hodell, D.A., 2018. Precession and atmospheric CO₂ modulated variability of sea ice in the central Okhotsk Sea since 130,000 years ago. *Earth Planet Sci. Lett.* 488, 36–45.
- Locarnini, R.A., Mishonov, A.V., Antonov, J.I., Boyer, T.P., Garcia, H.E., 2006. world ocean Atlas 2005, volume 1: temperature. In: Levitus, S. (Ed.), *NOAA Atlas NESDIS 61*. U.S. Government Printing Office, Washington D.C., p. 182
- Marchal, O., Cacheo, I., Stocker, T.F., Grimalt, J.O., Calvo, E., Martrat, B., Shackleton, N., Vautravers, M., Cortijo, E., van Kreveld, S., Andersson, C., Koc, N., Chapman, M., Sbaffi, L., Duplessy, J.C., Sarnthein, M., Turon, J.L., Duprat, J., Jansen, E., 2002. Apparent long-term cooling of the sea surface in the northeast Atlantic and Mediterranean during the Holocene. *Quat. Sci. Rev.* 21, 455–483.
- Max, L., Riethdorf, J.R., Tiedemann, R., Smirnova, M., Lembke-Jene, L., Fahl, K., Nürnberg, D., Matul, A., Mollenhauer, G., 2012. Sea surface temperature variability and sea-ice extent in the subarctic northwest Pacific during the past 15,000 years. *Paleoceanography* 27, PA3213.
- Max, L., Belz, L., Tiedemann, R., Fahl, K., Nürnberg, D., Riethdorf, J.R., 2014. Rapid shifts in subarctic Pacific climate between 138 and 70 ka. *Geology* 42, 899–902.
- Martinez-Garcia, A., Rosell-Mele, A., Geibert, W., Gersonde, R., Masque, P., Gaspari, V., Barbante, C., 2009. Links between iron supply, marine productivity, sea surface temperature, and CO₂ over the last 1.1 Ma. *Paleoceanography* 24, PA1207.
- Méheust, M., Fahl, K., Stein, R., 2013. Variability in modern sea surface temperature, sea ice and terrigenous input in the sub-polar North Pacific and Bering Sea: reconstruction from biomarker data. *Org. Geochem.* 57, 54–64.
- Meyer, V.D., Hefta, J., Lohmann, G., Max, L., Tiedemann, R., Mollenhauer, G., 2017. Summer temperature evolution on the Kamchatka peninsula, Russian far east, during the past 20 000 years. *Clim. Past* 13, 359–377.
- Müller, P.J., Kirst, G., Ruhland, G., von Storch, I., Rosell-Mele, A., 1998. Calibration of the alkenone paleotemperature index UK'37 based on core-tops from the eastern South Atlantic and the global ocean (60 degrees N - 60 degrees S). *Geochem. Cosmochim. Acta* 62, 1757–1772.
- Naafs, B.D.A., Stein, R., Hefta, J., Khelifi, N., De Schepper, S., Haug, G.H., 2010. Late pliocene changes in the north atlantic current. *Earth Planet. Sci. Lett.* 298, 434–442.
- Naafs, B.D.A., Hefta, J., Stein, R., 2013. Millennial-scale ice rafting events and hudson strait heinrich(-like) events during the late pliocene and pleistocene: a review. *Quat. Sci. Rev.* 80, 1–28.
- Nakatsuka, T., Fujimune, T., Yoshikawa, C., Noriki, S., Kawamura, K., Fukamachi, Y., Mizuta, G., Wakatsuchi, M., 2004. Biogenic and lithogenic particle fluxes in the western region of the Sea of Okhotsk: implications for lateral material transport and biological productivity. *Journal of Geophysical Research-Oceans* 109, C09S13.
- Niebauer, H.J., 1998. Variability in Bering Sea ice cover as affected by a regime shift in the North Pacific in the period 1947–1996. *Journal of Geophysical Research-Oceans* 103, 27717–27737.
- Nürnberg, D., Baranov, B.V., Karp, B.Y., 1997. GREGORY — German Russian Expedition for Geological/Geophysical Research, p. 69. GEOMAR Report No. 60, Kiel, Germany.
- Ohtani, K., Akiba, Y., Takenouti, A.Y., 1972. Formation of western subarctic water in the Bering Sea. In: Takenouti, A.Y. (Ed.), *Biological Oceanography of the Northern North Pacific Ocean*. Idemitsu Shoten Publ. Co, pp. 32–44.
- Prahl, F.G., Wakeham, S.G., 1987. Calibration of unsaturation patterns in long-chain ketone compositions for paleotemperature assessment. *Nature* 330, 367–369.
- Prahl, F.G., Muehlhausen, L.A., Zahnle, D.L., 1988. Further evaluation of long-chain alkenones as indicators of paleoceanographic conditions. *Geochem. Cosmochim. Acta* 52, 2303–2310.
- Prahl, F.G., Rontani, J.F., Zabeti, N., Walinsky, S.E., Sparrow, M.A., 2010. Systematic pattern in UK'37 – temperature residuals for surface sediments from high latitude and other oceanographic settings. *Geochem. Cosmochim. Acta* 74, 131–143.
- Ren, J., Gersonde, R., Esper, O., Sancetta, C., 2014. Diatom distributions in northern North Pacific surface sediments and their relationship to modern environmental variables. *Palaeogeogr. Palaeoclimatol. Palaeoecol.* 402, 81–103.
- Roden, G.I., Taft, B.A., Ebbesmeyer, C.C., 1982. Oceanographic aspects of the emperor seamounts region. *Journal of Geophysical Research-Oceans* 87, 9537–9552.
- Rontani, J.F., Harji, R., Guasco, S., Prahl, F.G., Volkman, J.K., Bhosle, N.B., Bonin, P., 2008. Degradation of alkenones by aerobic heterotrophic bacteria: selective or not? *Org. Geochem.* 39, 34–51.
- Rontani, J.F., Volkman, J.K., Prahl, F.G., Wakeham, S.G., 2013. Biotic and abiotic degradation of alkenones and implications for UK'37 paleoproxy applications: a review. *Org. Geochem.* 59, 95–113.
- Rosell-Melé, A., Eglington, G., Pflaumann, U., Sarnthein, M., 1995. Atlantic core-top calibration of the UK37 index as a sea-surface paleotemperature indicator. *Geochem. Cosmochim. Acta* 59, 3099–3107.
- Rosell-Melé, A., 1998. Interhemispheric appraisal of the value of alkenone indices as temperature and salinity proxies in high-latitude locations. *Paleoceanography* 13, 694–703.
- Rosell-Melé, A., Comes, P., Müller, P.J., Ziveri, P., 2000. Alkenone fluxes and anomalous U-UK'37 values during 1989–1990 in the Northeast Atlantic (48 degrees N 21 degrees W). *Mar. Chem.* 71, 251–264.
- Rosell-Melé, A., Prahl, F.G., 2013. Seasonality of UK'37 temperature estimates as inferred from sediment trap data. *Quat. Sci. Rev.* 72, 128–136.
- Schlitzer, R., 2015. Data analysis and visualization with ocean data view. *CMOS Bull. SCMO* 43 (1), 9–13.
- Seki, O., Ishiwatari, R., Matsumoto, K., 2002. Millennial climate oscillations in NE Pacific surface waters. *Geophys. Res. Lett.* 29 (23), 2144.
- Seki, O., Nakatsuka, T., Kawamura, K., Saitoh, S.I., Wakatsuchi, M., 2007. Time-series sediment trap record of alkenones from the western Sea of Okhotsk. *Mar. Chem.* 104, 253–265.
- Sekine, Y., 1988. Anomalous southward intrusion of the Oyashio east of Japan .1. Influence of the seasonal and interannual variations in the wind stress over the north pacific. *Journal of Geophysical Research-Oceans* 93, 2247–2255.
- Sikes, E.L., Farrington, J.W., Keigwin, L.D., 1991. Use of the alkenone unsaturation ratio UK37 to determine past sea-surface temperatures – core-top SST calibrations and methodology considerations. *Earth Planet Sci. Lett.* 104, 36–47.
- Sikes, E.L., Volkman, J.K., Robertson, L.G., Pichon, J.J., 1997. Alkenones and alkenes in surface waters and sediments of the Southern Ocean: implications for paleotemperature estimation in polar regions. *Geochem. Cosmochim. Acta* 61, 1495–1505.
- Sikes, E.L., O'Leary, T., Nodder, S.D., Volkman, J.K., 2005. Alkenone temperature records and biomarker flux at the subtropical front on the chatham rise, SW Pacific Ocean. *Deep Sea Res. Oceanogr. Res. Pap.* 52, 721–748.
- Sonzogni, C., Bard, E., Rostek, F., Lafont, R., Rosell-Melé, A., Eglington, G., 1997. Core-top calibration of the alkenone index vs sea surface temperature in the Indian Ocean. *Deep-Sea Res. Part II Top. Stud. Oceanogr.* 44, 1445–1460.
- Stabeno, P.J., Schumacher, J.D., Ohtani, K., 1999. The physical oceanography of the Bering Sea. In: Loughlin, T.R., Ohtani, K. (Eds.), *Dynamics of the Bering Sea*. University of Alaska Sea Grant Fairbanks, AK-SG-99-03, pp. 1–28.
- Ternois, Y., Kawamura, K., Ohkouchi, N., Keigwin, L., 2000. Alkenone sea surface temperature in the Okhotsk Sea for the last 15 kyr. *Geochem. J.* 34, 283–293.
- Tierney, J.E., Tingley, M.P., 2018. BAYSPLINE: a new calibration for the alkenone paleothermometer. *Paleoceanography and Paleoclimatology* 33, 281–301.
- Tsutsui, H., Takahashi, K., Asahi, H., Jordan, R.W., Nishida, S., Nishiaki, N.,

- Yamamoto, S., 2016. Nineteen-year time-series sediment trap study of *Coccolithus pelagicus* and *Emiliania huxleyi* (calcareous nannoplankton) fluxes in the Bering Sea and subarctic Pacific Ocean. Deep-Sea Res. Part II Top. Stud. Oceanogr. 125, 227–239.
- Villanueva, J., Grimalt, J.O., Cortijo, E., Vidal, L., Labeyrie, L., 1998. Assessment of sea surface temperature variations in the central North Atlantic using the alkenone unsaturation index UK'37. Geochim. Cosmochim. Acta 62, 2421–2427.
- Wang, Y.M.V., Leduc, G., Regenberg, M., Andersen, N., Larsen, T., Blanz, T., Schneider, R.R., 2013. Northern and southern hemisphere controls on seasonal sea surface temperatures in the Indian Ocean during the last deglaciation. Paleoceanography 28, 619–632.
- Yamamoto, M., Shiraiwa, Y., Inouye, I., 2000. Physiological responses of lipids in *Emiliania huxleyi* and *Gephyrocapsa oceanica* (Haptophyceae) to growth status and their implications for alkenone paleothermometry. Org. Geochem. 31, 799–811.
- Yamamoto, M., Oba, T., Shimamura, J., Ueshima, T., 2004. Orbital-scale anti-phase variation of sea surface temperature in mid-latitude North Pacific margins during the last 145,000 years. Geophys. Res. Lett. 31, L16311.
- Yamamoto, M., Shimamoto, A., Fukuhara, T., Naraoka, H., Tanaka, Y., Nishimura, A., 2007. Seasonal and depth variations in molecular and isotopic alkenone composition of sinking particles from the western North Pacific. Deep Sea Res. Oceanogr. Res. Pap. 54, 1571–1592.
- Yang, J.Y., Honjo, S., 1996. Modeling the near-freezing dichothermal layer in the Sea of Okhotsk and its interannual variations. Journal of Geophysical Research-Oceans 101, 16421–16433.